Structural, magnetic and transport properties of single-crystalline U_2Pt_2In

1998 J. Phys.: Condens. Matter 10 9465

(http://iopscience.iop.org/0953-8984/10/42/012)

J. Phys.: Condens. Matter **10** (1998) 9465–9475. Printed in the UK PII: S0953-8984(98)95836-2

Structural, magnetic and transport properties of single-crystalline U_2Pt_2In

P Estrela†‡¶, L C J Pereira§, A de Visser†, F R de Boer†, M Almeida§, M Godinho‡, J Rebizant‖ and J C Spirlet‖[+]

† Van der Waals—Zeeman Instituut, Universiteit van Amsterdam, Valckenierstraat 65, NL-1018 XE Amsterdam, The Netherlands

‡ Departamento de Física, Faculdade de Ciências da Universidade de Lisboa, Campo Grande ed. C1, P-1700 Lisboa, Portugal

§ Departamento de Química, Instituto Tecnológico e Nuclear, P-2686 Sacavém Codex, Portugal

‖ European Commission, Joint Research Centre, Institute for Transuranium Elements, Postfach 2340, D-76125 Karlsruhe, Germany

Received 13 July 1998

Abstract. Single crystals of the heavy-electron compound U_2Pt_2In have been grown by a modified mineralization technique. The x-ray structure refinement shows that U_2Pt_2In single crystals form in the Zr_3Al_2 structure, instead of the U_3Si_2 structure reported for polycrystalline material. The polymorphism of U_2Pt_2In is attributed to the experimental parameters, such as pressure and temperature, during the sample preparation process. The single-crystal susceptibility data reveal a weak maximum for χ_c at $T_{max} = 7.9$ K, indicating the presence of short-range antiferromagnetic correlations, while χ_a has the tendency to diverge at low $T (T > 2$ K). The electrical resistivity of the single crystals ($T > 0.3$ K) is best described by $\rho \sim T^{\alpha}$ with $\alpha \sim 1.1(1)$ for $I \parallel a$ and $\alpha \sim 0.3(2)$ for $I \parallel c$. The magnetic and transport data show pronounced deviations from the standard Fermi-liquid picture, and lead to a classification of U_2Pt_2In as a non-Fermi-liquid compound. As the origin of NFL behaviour in U_2Pt_2In we propose the proximity to a quantum critical point or Kondo disorder.

1. Introduction

The family of U_2T_2X (where T is a transition metal and X is In or Sn) intermetallic compounds has attracted much interest in the past years [1–3], because it may serve as an exemplary system to study hybridization phenomena in 5f electron compounds. The hybridization strength can be tuned by varying the T and X elements and as a result various magnetic ground states are observed, notably Pauli paramagnetism, spin-fluctuation phenomena and antiferromagnetism. The shortest uranium–uranium distance in these 2:2:1 compounds is close to the Hill limit (~ 3.5 Å) and is found either along the *c*-axis or within the *ab*-plane. This enables the study of the influence of the direct f–f coupling on the magnetic f-moment direction. On the other hand, the strength of the 5f–d ligand

¶ Corresponding author: P Estrela, Van der Waals–Zeeman Institute, University of Amsterdam, Valckenierstraat 65, 1018 XE Amsterdam, The Netherlands. E-mail address: estrela@phys.uva.nl.

[+] Present address: European Commission, Joint Research Centre, IRMM, Retieseweg, B-2440 Geel, Belgium.

0953-8984/98/429465+11$19.50

hybridization is the parameter which controls the evolution of magnetism across the 2:2:1 series (see [4] for In and Sn compounds).

The U_2T_2X compounds crystallize in the tetragonal U_3Si_2-type structure (space group $P4/mbm$) [1], except for U_2Pt_2Sn [5] and U_2Ir_2Sn [6], which crystallize in the Zr_3Al_2-type structure (space group $P4_2/mnm$). The Zr_3Al_2-type structure is a superstructure (doubling of the c-axis) of the U_3Si_2-type structure. Within a systematic study of the structural and physical properties of the An_2T_2X series, single crystals of several uranium 2:2:1 compounds were grown [7]. In this paper we focus on U_2Pt_2In, which has a number of unrivalled properties. We found that, while our polycrystalline samples form in the U_3Si_2-type structure, the single crystals form in the Zr_3Al_2 superstructure. Polycrystalline U_2Pt_2In was classified as a non-ordering heavy-electron compound [2]. Our recent low-temperature specific-heat, magnetization and resistivity studies, carried out on single-crystalline material, confirm the heavy-electron behaviour, but moreover reveal pronounced deviations from the standard Fermi-liquid picture, thereby classifying U_2Pt_2In as a non-Fermi-liquid compound.

The heavy-electron properties of U_2Pt_2In were first reported by Havela *et al* [2]. Specific-heat experiments carried out on a polycrystalline sample of U_2Pt_2In [2, 3] in the temperature range 1.3–40 K revealed the presence of a pronounced upturn of the electronic specific heat divided by temperature (c/T) below $T \approx 8$ K, insensitive to an applied field of 5 T. The $c(T)$ data could be fitted with a $T^3 \ln T$ term below 5 K, providing evidence for spin-fluctuation phenomena. The resulting linear coefficient of the electronic specific heat $\gamma(T \to 0\ \text{K})$ amounts to 415 mJ mol_U^{-1} K^{-2}, which classifies U_2Pt_2In as a heavy-electron compound. In line with this, the electrical resistivity, $\rho(T)$, of U_2Pt_2In shows a weak maximum around 80 K and coherence effects at low temperatures, which can be attributed to the Kondo-lattice effect. The magnetic susceptibility, $\chi(T)$, shows deviations from the Curie–Weiss behaviour below ~ 150 K. In the limit $T \to 1.2$ K, χ is enhanced and continues to rise. No sign of magnetic ordering has been observed.

More recently, data taken on a polycrystalline sample [8] showed that $\rho(T) = \rho_0 + bT$ in the temperature range 1.4–6 K. This led to the suggestion [8] that U_2Pt_2In might be a good candidate to study non-Fermi-liquid (NFL) phenomena. The most prominent features of an NFL [9] are a specific heat which varies as $c(T) \sim -T \ln T$, a low-temperature divergency of $\chi(T)$ and a resistivity which varies as $\rho(T) \sim T^\alpha$ (where $\alpha = 1$ or 0.5). There are several mechanisms which may lead to NFL effects, like the proximity to a quantum phase transition, the two-channel Kondo effect and Kondo disorder. As NFL effects nowadays attract much attention, it is of interest to study the thermal, transport and magnetic properties of single-crystalline U_2Pt_2In at lower temperatures ($T < 1.2$ K).

In this paper we report on the crystal growth of U_2Pt_2In and the characterization of the grown crystals by x-ray diffraction and magnetization and resistivity experiments.

2. Experiment

2.1. Single-crystal growth

The starting material was prepared by arc melting the quasi-stoichiometric amounts of the elements with a purity better than 99.9% (U) and 99.999% (Pt, In) in a water-cooled copper crucible under a purified argon atmosphere. A small excess of In was added in order to compensate for evaporation losses. The mass loss after arc melting was less than 0.5%. The x-ray analysis, optical microscopy and secondary electron microscopy (SEM) showed that the arc melted material was single-phase.

The polycrystalline batch (mass $\sim$ 20 g) was encapsulated in a tungsten crucible and sealed by electron-beam welding under vacuum (2×10^{-5} atm). The crystals were grown by a modified mineralization technique [7] using radiofrequency heating with an *in situ* temperature reading in order to control the melting temperature plateau (1380–1335 °C). The *in situ* temperature reading made it possible to reduce the mineralization time significantly, from a typical 1 week to 5 hours only. The single-phase character of the grown U_2Pt_2In material was checked by x-ray diffraction, optical microscopy and SEM.

2.2. Characterization techniques

The structural aspects of the polycrystalline and single-crystalline material were investigated by x-ray diffraction. In the case of the polycrystalline material x-ray powder diffraction was carried out on a Philips PW1120/90 generator using Cu Kβ radiation filtered out by Ni. The crystallinity of the single crystals was checked by the back-reflection Laue method on a Philips PW1120/90 generator with Cu Kβ radiation filtered out by Ni. Diffraction images were collected on Polaroid ISO3000/36° films. The lattice parameters and the atomic positions were determined by single-crystal x-ray diffraction on an Enraf–Nonius four circle CAD-4 diffractometer with graphite-monochromated Mo Kα radiation ($\lambda = 0.7093$ Å) and the $\omega - 2\theta$ scan technique with $\Delta\omega = 0.90 + 0.35 \tan\theta$.

Magnetization measurements were performed on several single crystals (with a mass of 10–50 mg) using a SQUID magnetometer (Quantum Design) in the temperature range 2–350 K and in applied fields up to 5.5 T. In addition, magnetization measurements were carried out in high magnetic fields up to 35 T at $T = 4.2$ K in the Amsterdam High Field Facility.

Resistivity measurements were carried out on bar-shaped crystals, for a current along the *a*- and *c*-axis, in the temperature range 0.3–12 K using a ^{3}He system. A standard a.c. four-point method was used with an excitation current of the order of 300 μA. The excitation current was varied in order to check for heating effects.

3. Experimental results and analysis

3.1. X-ray diffraction

The x-ray powder diffraction data taken on polycrystalline U_2Pt_2In confirmed the U_3Si_2-type structure (space group $P4/mbm$). This structure has two formula units per unit cell ($Z = 2$). The lattice parameters were determined as $a = 7.654$ Å and $c = 3.725$ Å in good agreement with the literature [1].

On several pieces of single-crystalline material a complete structural analysis was carried out on the Enraf–Nonius four circle CAD-4 diffractometer. The lattice parameters were obtained by least-squares refinement of the setting angles of 24 reflections using the Enraf–Nonius CAD-4 package. The intensities of three standard reflections were measured at intervals of 2 hours and anisotropic decay corrections were applied to the data. Absorption corrections were applied on the basis of ψ scan data obtained from five reflections. The crystallographic calculations were made using the SDP program package [10]. Details of the intensity data collection and crystallographic data for U_2Pt_2In are summarized in tables 1 and 2. From these data it follows that our U_2Pt_2In single crystals form in a different structure than the polycrystalline material, namely the tetragonal Zr_3Al_2 type of structure (space group $P4_2/mnm$). This structure has four formula units per unit cell ($Z = 4$).

Table 1. Crystallographic data for U_2Pt_2In single crystals.

Chemical formula	U_2Pt_2In
Formula weight (g mol^{-1})	981.06
Crystal system	tetragonal
Space group	$P4_2/mnm$ (No 136)
a (Å)	7.6946(3)
c (Å)	7.3676(3)
V (Å^3)	436.21(5)
Z	4
Number of reflections for LS cell parameters	24
θ range for LS cell parameters	7.67–17.87
D_{calc} (g cm^{-3})	14.938
Approximate crystal dimensions (mm^3)	$0.05 \times 0.04 \times 0.83$
Radiation, wavelength (Å)	Mo Kα, 0.709 30
Monochromator	graphite
Temperature (K)	297 K
θ range (°)	2–30
ω-2θ scan	$\Delta\omega = 0.90 + 0.35 \tan\theta$
Data set	$-10 \leqslant h \leqslant 10$; $-10 \leqslant k \leqslant 10$; $-10 \leqslant l \leqslant 0$
Total data	2705
Unique data	380
Observed data ($I \geqslant 3\sigma(I)$)	298
Decay corrections (min/max)	0.9507/1.0250
Number of reflections	5
θ range for Ψ scan absorption corrections	8.11–16.10
Transmission factors (min/max)	23.10/99.13
μ (Mo Kα) (cm^2 g^{-1})	1397.077
Number of refined parameters	7
Final agreement factors[a]	
$R = \sum \|F_{obs} - F_{calc}\| / \sum \|F_{obs}\|$	0.0427
$wR = \{\sum[w(\|F_{obs}\| - \|F_{calc}\|)^2] / w\|F_{obs}\|^2\}^{1/2}$	0.0655
$S = [\sum w(\|F_{obs}\| - \|F_{calc}\|)^2/(m-n)]^{1/2}$	1.742

[a] m, number of observations; n, number of variables.

Table 2. Positional parameters and anisotropic temperature factors (10^{-4} Å^2) of U_2Pt_2In single crystals.

Atom	Position	x	y	z	$U_{11} = U_{22}$	U_{33}	U_{12}
U	4f	0.335 37	0.335 37	0	15	30	1.2
U	4g	0.180 35	−0.180 35	0	25	24	26
Pt	8j	0.130 13	0.130 09	0.234 53	20	41	−10
In	4d	0	1/2	−1/4	24	70	0

The lattice parameters are: $a = 7.695$ Å and $c = 7.368$ Å. In the Zr_3Al_2-type structure the U atoms occupy two different crystallographic positions: 4f (x_1, x_1, 0) and 4g (x_2, $-x_2$, 0). The X atoms are on the 4d (0, 1/2, 1/4) positions and the T atoms on the 8j (x_3, x_3, y) positions. The average values of x_1, x_2, x_3 and y are 0.335, 0.180, 0.130 and 0.235, respectively. A schematic view of the unit cell is presented in figure 1. Interatomic bonding distances and nearest neighbour positions, calculated for the U_2Pt_2In single crystals, are listed in table 3.

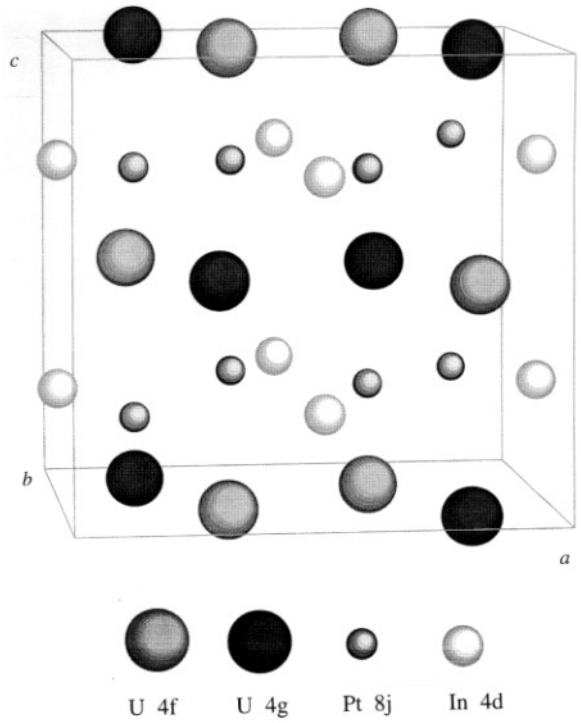

Figure 1. Unit cell of U_2Pt_2In (crystallographic structure of the Zr_3Al_2-type, $P4_2/mnm$).

Table 3. Interatomic bonding distances and nearest neighbours of U_2Pt_2In single crystals.

Atom	NN	Atom	d (Å)	Atom	NN	Atom	d (Å)
U (4f)	1	U (4f)	3.583	U (4g)	2	U (4f)	3.687
	2	U (4g)	3.687		2	U (4f)	3.913
	2	U (4g)	3.913		2	U (4f)	4.144
	2	U (4g)	4.144		1	U (4g)	3.925
	2	Pt (8j)	2.828		2	Pt (8j)	2.838
	4	Pt (8j)	3.013		4	Pt (8j)	2.975
	4	In (4d)	3.414		4	In (4d)	3.372
Pt (8j)	1	U (4f)	2.828	In (4d)	4	U (4f)	3.414
	2	U (4f)	3.013		4	U (4g)	3.372
	1	U (4g)	2.838		4	Pt (8j)	3.019
	2	U (4g)	2.975		2	In (4d)	3.684
	1	Pt (8j)	2.832				
	1	Pt (8j)	3.456				
	2	In (4d)	3.019				

3.2. Magnetization and susceptibility

The temperature variation of the susceptibility, $\chi_a(T)$ and $\chi_c(T)$, where a and c refer to the crystallographic direction along which the magnetic field ($B = 0.05$ and 0.1 T) is applied, is presented in figure 2. The susceptibility is anisotropic, with the c-axis as the easy axis for magnetization. This anisotropy persists in the whole temperature range (up to 350 K).

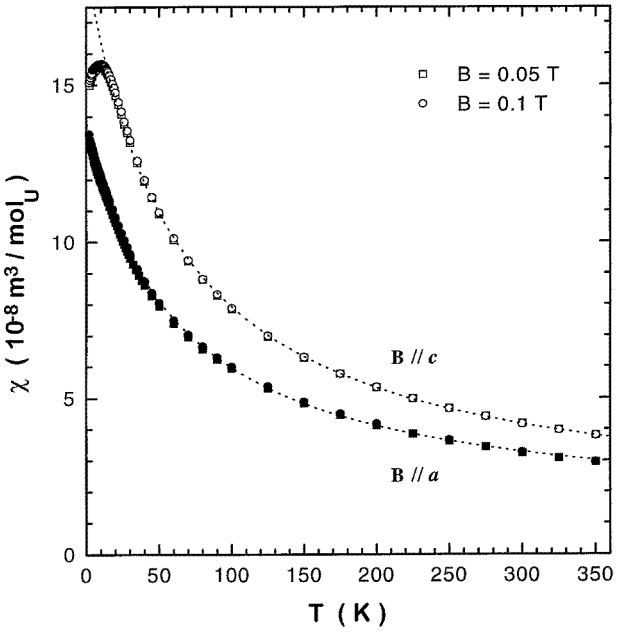

Figure 2. Temperature dependence of the susceptibility for magnetic fields of 0.05 (squares) and 0.1 T (circles) applied along the crystallographic *a*- (full symbols) and *c*-axis (open symbols). The lines represent modified Curie–Weiss laws (see text).

At low temperatures, a clear difference between χ_a and χ_c is observed. χ_a continues to increase as the temperature is lowered down to 2 K, while χ_c displays a broad maximum below 10 K (figure 2). Tracing the derivatives, $\mathrm{d}\chi/\mathrm{d}T$, shows that the maximum occurs at $T_{\max} = 7.9(3)$ K. The relative height and width of the maximum do not change significantly with the applied field strength (from 0.005 to 5.5 T). This type of behaviour is frequently observed in systems which exhibit exchange enhanced Pauli paramagnetism [11]. The maximum in χ_c is indicative of the stabilization of short-range antiferromagnetic correlations along the *c*-axis.

Above 10 K, the susceptibility follows a modified Curie–Weiss law, $\chi = \chi_0 + C/(T-\theta)$. For $B \parallel c$ we obtain the parameters $\chi_0 = 1.1 \times 10^{-8}$ m^3 mol$_U^{-1}$, $\theta = -62$ K and $\mu_{\mathrm{eff}} = 2.6\ \mu_B$/U, while for $B \parallel a$ we obtain $\chi_0 = 1.1 \times 10^{-8}$ m^3 mol$_U^{-1}$, $\theta = -63$ K and $\mu_{eff} = 2.2\ \mu_B$/U. The fitted Curie–Weiss behaviour is represented by the dashed lines in figure 2. The near-equality of the paramagnetic Pauli temperatures θ reflects the weak anisotropy in this system. These results compare to the following parameters obtained on polycrystalline material: $\chi_0 = 4.9 \times 10^{-8}$ m^3 mol$_U^{-1}$, $\theta = -106$ K and $\mu_{\mathrm{eff}} = 2.4\ \mu_B$/U [2]. The μ_{eff} values are considerably reduced from the free-ion value for U^{3+} and U^{4+}, 3.62 μ_B and 3.58 μ_B, respectively, which points to a strong hybridization of the f electrons and the conduction band.

The magnetization $M_a(B)$ and $M_c(B)$ is shown in figure 3 at some selected temperatures. The magnetization is linear in fields up to 5.5 T and the slope $\mathrm{d}M/\mathrm{d}B$ is always higher for $B \parallel c$ than for $B \parallel a$. $M(T = 2\ \mathrm{K})$ reaches the value of 0.25 (0.21) μ_B fu^{-1} for a field of 5.5 T along the $c(a)$ axis. No hysteresis in M_a and M_c was observed. Magnetization measurements for $B \parallel c$ at 4.2 K were carried out up to 35 T. No significant deviation from a linear behaviour was observed. In the maximum field $M_c(35\ \mathrm{T}) = 1.48\ \mu_B$ fu^{-1}.

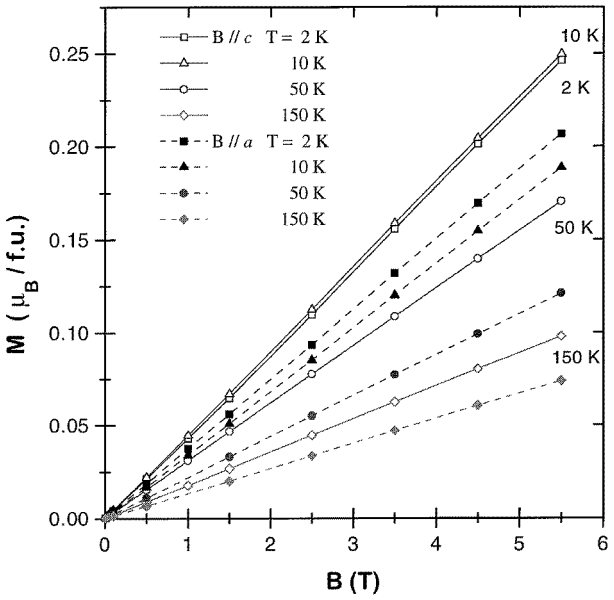

Figure 3. Field dependence of the magnetization along the a- (full symbols and dotted lines) and c-axis (open symbols, full lines) at different temperatures.

These results are similar to the ones obtained on polycrystalline samples up to 35 T [12] and 57 T [13]. In the polycrystalline data a weak nonlinearity was observed, which was not found in the single-crystal data. The nonlinearity is possibly due to the saturation of magnetic impurities in the polycrystalline sample (about 2% UPt was present as a second phase [3]). The data for free and fixed powder are identical which is another indication that the magnetic anisotropy is rather weak in this compound.

The magnetization and susceptibility data do not show any sign of long-range magnetic order in U_2Pt_2In down to 2 K. Zero-field μSR experiments carried out on poly- and single-crystalline material confirm the absence of magnetic order [14]. We have also searched for spin-glass effects. Susceptibility data obtained after zero-field cooling (ZFC) and field cooling (FC) are identical, hence we do not find any signals of a spin-glass ground state.

3.3. Resistivity

The resistance curves for $I \parallel a$ and $I \parallel c$ are shown in figure 4 for $T < 10$ K. The $R(T)$ values are normalized to R(300 K). For both $I \parallel a$ and $I \parallel c$, the resistivity $\rho_{a,c}$(300 K) amounts to 220 ± 20 $\mu\Omega$ cm. The experimental error in $\rho_{a,c}$(300 K) is mainly due to the uncertainty in the determination of the distance between the voltage contacts. Upon cooling, $\rho_{a,c}(T)$ starts to rise and a weak maximum is observed just below nitrogen temperature. As can be seen in figure 4, the resistivity is anisotropic: $\rho_c > \rho_a$. For $I \parallel c$ the resistivity decreases very slowly with decreasing temperature down to $\sim$3 K, after which it starts to decrease more rapidly. For $I \parallel a$ the resistivity decreases somewhat faster than for $I \parallel c$ down to $\sim$4 K. Below $T = 3.7$ K, ρ_a follows the expression $\rho_a = \rho_{0,a} + b_a T$. For $I \parallel c$ an approximate linear temperature variation is observed below $T = 1.2$ K. $\rho_{0,a}$ and $\rho_{0,c}$

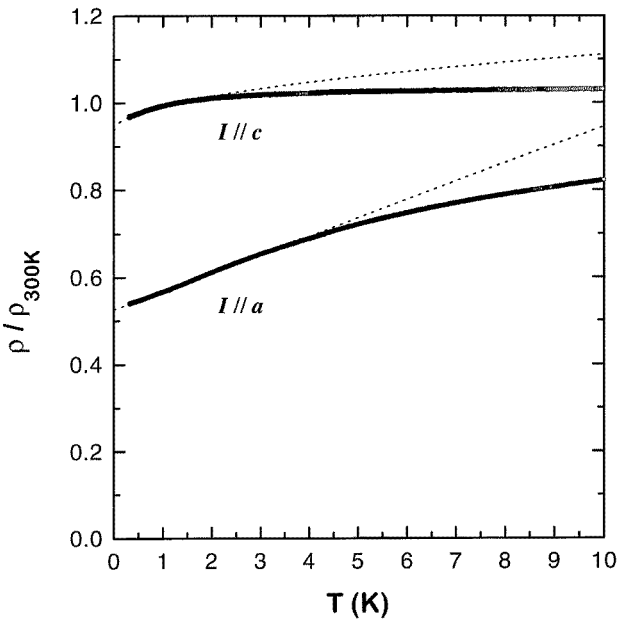

Figure 4. Zero-field normalized resistivity for currents applied along the a- and c-axis. The lines are low-temperature fits to $\rho_a \sim T$ and $\rho_c \sim \sqrt{T}$ (see text).

equal 110 and 200 $\mu\Omega$ cm, respectively, while b_a and b_c amount both to $\sim$8.5 $\mu\Omega$ cm K^{-1}. This linear temperature dependence, previously reported for a polycrystalline sample [8] in the temperature range 1.4–10 K, is one of the characteristic features of non-Fermi-liquid behaviour.

A closer inspection of the resistivity curves shows, however, that a better description can be given by the power law $\rho \sim 1 + a(T/T_0)^{\alpha}$, where T_0 is a characteristic temperature often identified with the Kondo temperature [9]. In order to determine the exponent which best describes the resistivity curves, least squares fits were performed using the data from the lowest temperature (0.3 K) up to a temperature T'. Tracing the goodness of fit for T' between 0.5 K and 4.2 K in steps of 0.1 K, one can choose the temperature range where the power law applies best. The exponents obtained were $\alpha_a = 1.1(1)$ below $T' = 2.6$ K and $\alpha_c = 0.3(2)$ below $T' = 2.3$ K, where the errors in $\alpha_{a,c}$ reflect the uncertainty in choosing T'. Thus for $I \parallel a$ the low-temperature resistivity varies approximately linearly in T, while the resistivity along the c direction is best described by a term of the order $\sqrt{T}$ (see figure 4).

4. Discussion

The polymorphism of U_2Pt_2In shows that the stability of the crystallographic structure depends on the experimental conditions, like pressure and temperature, during the sample preparation process. By preparing the arc melted polycrystalline sample, the temperatures attained are well above the melting point of U_2Pt_2In and the cooling process is rather fast. This leads to the formation of the U_3Si_2-type structure, which might not be the most stable

one, since the thermodynamic conditions during arc melting are not well defined equilibrium conditions. During the single-crystal growth, i.e. the mineralization process, the temperature range is much reduced (up to 20 °C above the melting point) and the cooling takes place very slowly. Under these conditions closer to equilibrium, the preferred structure is the tetragonal Zr_3Al_2-type structure. This structure was found in two other members of the U_2T_2X family, namely U_2Pt_2Sn and U_2Ir_2Sn (polycrystalline samples) [5, 6]. The tetragonal Zr_3Al_2-type structure is a superstructure (doubling of the c-axis) of the tetragonal U_3Si_2-type. This latter structure was reported for the majority of the U 2:2:1 compounds [1, 15] and all Np [1, 7], Pu and Am [16] 2:2:1 compounds.

The inter-uranium distances, reported in table 3, are slightly above the Hill limit (∼3.5 Å) for uranium [17]. From this, one may conjecture that U_2Pt_2In orders magnetically, as it is located on the magnetic side in the Hill plot. However, in the past decade it has become clear that the hybridization in many uranium compounds is governed by the 5f–d ligand overlap and that the Hill-limit picture is too simple. Recently, *ab initio* calculations using an optimized linear combination of atomic orbitals method, based on the local density approximation (LDA) [18, 19], show that the electronic structure and related properties of the U_2T_2X compounds mainly originate from the interplay between the band filling of the transition metal d states and the f states of the uranium atoms, with a decrease of the f–d hybridization when filling up the d bands. Within a simple tight-binding model based on the LDA approximation [4] it can also be shown that the evolution of magnetism across the 2:2:1 series (for In and Sn compounds) is related to the strength of the 5f–d ligand hybridization. In the U_2T_2In series, U_2Pd_2In and U_2Ni_2In order antiferromagnetically with Néel temperatures of 38 and 14 K, respectively, whereas for U_2Co_2In and U_2Rh_2In the ground state is paramagnetic (at least down to 1.2 K). When tracing the magnetic ordering temperatures of the In and Sn 2:2:1 compounds versus the square of the calculated hybridization matrix elements a Doniach-like phase diagram results [20]. Interestingly, U_2Pt_2In is close to the magnetic/non-magnetic border line.

The participation of 5f electrons in the bonding in light-actinide intermetallics leads to a compression of the 5f charge densities towards the bonding directions, which are given primarily by the shortest inter-actinide directions [21]. In the UTX (1:1:1) family it was found that the magnetic moment is always directed perpendicular to the nearest U–U direction. However, exceptions to this rule have been found in the 2:2:1 family. In U_2Rh_2Sn [22] and U_2Co_2Sn [23], the shortest U–U distance is located along the c-axis and yet the uranium moments are aligned along c. In the case of U_2Pt_2In, the shortest U–U distance is located in the tetragonal plane. The susceptibility data show that the antiferromagnetic correlations (of the Ising type) are found along the c-axis. This complies with the shortest f–f distance rule, as reported for the 1:1:1 compounds.

The analysis of the resistivity leads to a description with a low-temperature term $T^{\alpha}(T \to 0\ \mathrm{K})$, with $\alpha = 1.1(1)$ and 0.3(2) for the a- and c-axis, respectively. The absence of the usual Fermi-liquid T^2 term gives strong support for non-Fermi-liquid behaviour in U_2Pt_2In. Recently, we have carried out specific-heat measurements on a single crystal down to 0.1 K [14] and found a clear logarithmic divergency of c/T below ∼6 K, i.e. over almost two decades of temperature. This puts the NFL behaviour in U_2Pt_2In on a firm footing. From the analysis of the specific heat, $c/T \sim (-1/T_0)\ln(T/T_0)$, we deduce the scaling temperature $T_0 = 22$ K. Using this value for T_0, the coefficient a of the power law in the resistivity can be calculated. We obtain $a = 2.27$ and 0.23 for $I \parallel a$ and $I \parallel c$, respectively. The value of T_0 is close to the Kondo temperature $T_K \sim 20$ K, which can be deduced from the susceptibility data, assuming that the paramagnetic Curie temperature θ is three to four times larger than T_K [24].

The unusual low-temperature susceptibility data yield further support for NFL behaviour. The theoretical expressions for the magnetic susceptibility of an NFL were evaluated as $\chi \sim -\ln T$ or $\chi \sim -\sqrt{T}$, depending on the type of system. $\chi_c(T)$ is dominated by antiferromagnetic correlations below ∼10 K, therefore, no non-analytical analysis can be done confidently. However, $\chi_a(T)$ continues to rise, at least down to $T = 2$ K. Analysing $\chi_a(T < 10\ \text{K})$ with a term $\chi_a \sim 1 - b(T/T_0)^\beta$ one finds $\beta = 0.7$ and $b = 0.24$, but the limited temperature range where this behaviour occurs, does not allow for an accurate estimate of the exponent β.

Forthcoming work should focus on identifying the origin of the NFL behaviour. A interesting scenario is the proximity of U_2Pt_2In to a quantum critical point [25]. This is reflected in the location of U_2Pt_2In at the border line between magnetic and non-magnetic compounds in a Doniach type of diagram for the U_2T_2X series (X = In, Sn). Tuning the quantum critical point with an external parameter, e.g. a magnetic field or (chemical) pressure, should elucidate the applicability of this scenario. An alternative mechanism which can lead to NFL behaviour is the Kondo disorder model [26] where the Kondo effect on each f-electron atom sets a different temperature scale, resulting in a broad range of effective Fermi temperatures. One should note that the residual resistivity values of our U_2Pt_2In single crystals are large, $\rho_{0,a}$ and $\rho_{0,c}$ equal 110 and 200 $\mu\Omega$ cm, respectively, which indicates that some disorder is present in the crystals. The origin of this disorder is unclear. The single-crystal x-ray structure refinement with a final agreement factor of 4.3%, is considered to indicate a high crystalline quality. However, a small percentage of site inversion (Pt and In inversion) can not be excluded. It is also possible that the disorder is somehow related to the polymorphism of U_2Pt_2In. On the other hand, preliminary magnetoresistance experiments [27] show a variation of $\rho_{0,a}$ and $\rho_{0,c}$ in field, which indicates that at least part of ρ_0 is caused by scattering mechanisms other than scattering at crystallographic defects. A more thorough characterization of the crystallinity of the sample, by e.g. neutron diffraction, is in progress.

5. Summary

Single crystals of the heavy-electron compound U_2Pt_2In have been grown by a modified mineralization technique. The single-crystal x-ray structure refinement shows that our U_2Pt_2In single crystals form in the Zr_3Al_2 structure, instead of forming in the U_3Si_2 structure reported for polycrystalline material. The polymorphism of U_2Pt_2In shows that the stability of the crystallographic structure depends on the experimental conditions, like pressure and temperature, during the sample preparation process.

Susceptibility data show pronounced deviations from a modified Curie–Weiss behaviour at low temperatures. χ_c exhibits a maximum at $T_{\max} = 7.9$ K, indicating the presence of short-range antiferromagnetic correlations. χ_a continues to rise down to the lowest temperatures ($T > 2$ K) with no evidence towards saturation. The electrical resistivity of the single crystals ($T \to 0$ K) is best described by $\rho \sim T^\alpha$ with $\alpha \sim 1.1(1)$ for $I \parallel a$ and $\alpha \sim 0.3(2)$ for $I \parallel c$. The magnetic and transport data show pronounced deviations from the standard Fermi-liquid picture, and lead to a classification of U_2Pt_2In as a non-Fermi-liquid compound. This is strongly supported by specific-heat experiments [14]. A logarithmic divergency of c/T is observed in the temperature interval 0.1–6 K. The location of U_2Pt_2In close to the magnetic/non-magnetic border line in a Doniach-type phase diagram suggests that a quantum phase transition is at the origin of the NFL behaviour. However, the Kondo-disorder scenario, as an alternative route to NFL behaviour in U_2Pt_2In, should be investigated as well.

Acknowledgments

P Estrela acknowledges the European Commission for a Marie Curie fellowship obtained within the TMR programme (contract No ERBFMBICT961763). This work was partially supported in Portugal by PRAXIS under contract Nos 2/2.1/QUI/202/94 and 3/3.1/FIS/29/94.

References

[1] Péron M N *et al* 1993 *J. Alloys Compounds* **201** 203
[2] Havela L *et al* 1994 *J. Appl. Phys.* **76** 6214
[3] Nakotte H 1994 *PhD Thesis* University of Amsterdam
[4] Prokeš K, Brück E, Nakotte H, de Châtel P F and de Boer F R 1995 *Physica* B **206/207** 8
[5] Gravereau P, Mirambet F, Chevalier B, Weill F, Fournès L, Laffargue D, Bourée F and Etourneau J 1994 *J. Mater. Chem.* **4** 1893
[6] Pereira L C J, Winand J M, Wastin F, Rebizant J and Spirlet J C 1994 *Proc.24th Journées des Actinides (Obergurgl)* p 109
[7] Pereira L C J 1998 *PhD Thesis* University of Lisbon
[8] Strydom A M and du Plessis P V 1997 *Physica* B **230–232** 62
[9] See e.g.: 1996 *Proc. ITP Workshop on Non-Fermi-Liquid Behaviour in Solids (Santa Barbara), J. Phys.: Condens. Matter* **8**
[10] Frenz B A 1986 *Ver. SDPPlus* V1.0 (Delft: Enraf-Nonius)
[11] Béal-Monod M T 1982 *Physica* B **109/110** 1837
[12] Nakotte H, Prokeš K, Brück E, Tang N, de Boer F R, Svoboda P, Sechovský V, Havela L, Winand J M, Seret A, Rebizant J and Spirlet J C 1994 *Physica* B **201** 247
[13] Fukushima T, Matsuyama S, Kumada T, Kindo K, Prokeš K, Nakotte H, de Boer F R, Havela L, Sechovský V, Winand J M, Rebizant J and Spirlet J C 1995 *Physica* B **211** 142
[14] Estrela P, de Visser A, de Boer F R, Nieuwenhuys G J, Pereira L C J and Almeida M *Proc. SCES'98, Physica* B submitted
[15] Mirambet F, Gravereau P, Chevalier B, Trut L and Etourneau J 1993 *J. Alloys Compounds* **203** 29
[16] Pereira L C J, Wastin F, Winand J M, Kanellakopoulos B, Rebizant J, Spirlet J C and Almeida M 1997 *J. Solid State Chem.* **134** 138
[17] Hill H H 1970 *Plutonium and Other Actinides 1970* ed W N Miner (New York: AIME) p 2
[18] Diviš M, Richter M and Eschrig H 1994 *Solid State Commun.* **90** 99
[19] Diviš M, Olšovec M, Richter M and Eschrig H 1995 *J. Magn. Magn. Mater.* **140–144** 1365
[20] Tran V H, Zolnierek Z, Zaleski A J and Noël H 1997 *Solid State Commun.* **101** 709
[21] Sechovský V, Havela L, Nakotte H, de Boer F R and Brück E 1994 *J. Alloys Compounds* **207/208** 221
[22] Pereira L C J, Paixão J A, Estrela P, Godinho M, Boudarot F, Bonnet M, Rebizant J, Spirlet J C and Almeida M 1996 *J. Phys.: Condens. Matter* **8** 11 167
[23] Paixão J A, Pereira L C J, Estrela P, Godinho M, Almeida M, Paolasini L, Bonnet M and Rebizant J 1998 *J. Phys.: Condens. Matter* submitted
[24] Brandt N B and Moshchalkov V V 1984 *Adv. Phys.* **33** 373
[25] Millis A J 1993 *Phys. Rev.* B **48** 7183
[26] Miranda E, Dobrosavljevic V and Kotliar G 1996 *J. Phys.: Condens. Matter* **8** 9871
[27] Estrela P, de Visser A, de Boer F R and Pereira L C J unpublished